CRYSTAL GROWTH & DESIGN

Subscriber access provided by NORTHERN KENTUCKY UNIV STEELY

Article

Orientation of Organic Cations in Hybrid Inorganic-Organic Perovskite CH3NH3PbI3 from Sub-atomic Resolution Single Crystal Neutron Diffraction Structural Studies

Yixin Ren, Iain W.H. Oswald, Xiaoping Wang, Gregory T. McCandless, and Julia Y Chan

Cryst. Growth Des., **Just Accepted Manuscript** • DOI: 10.1021/acs.cgd.6b00297 • Publication Date (Web): 30 Mar 2016

Downloaded from http://pubs.acs.org on April 9, 2016

Just Accepted

"Just Accepted" manuscripts have been peer-reviewed and accepted for publication. They are posted online prior to technical editing, formatting for publication and author proofing. The American Chemical Society provides "Just Accepted" as a free service to the research community to expedite the dissemination of scientific material as soon as possible after acceptance. "Just Accepted" manuscripts appear in full in PDF format accompanied by an HTML abstract. "Just Accepted" manuscripts have been fully peer reviewed, but should not be considered the official version of record. They are accessible to all readers and citable by the Digital Object Identifier (DOI®). "Just Accepted" is an optional service offered to authors. Therefore, the "Just Accepted" Web site may not include all articles that will be published in the journal. After a manuscript is technically edited and formatted, it will be removed from the "Just Accepted" Web site and published as an ASAP article. Note that technical editing may introduce minor changes to the manuscript text and/or graphics which could affect content, and all legal disclaimers and ethical guidelines that apply to the journal pertain. ACS cannot be held responsible for errors or consequences arising from the use of information contained in these "Just Accepted" manuscripts.

ACS Publications

Crystal Growth & Design is published by the American Chemical Society. 1155 Sixteenth Street N.W., Washington, DC 20036

Published by American Chemical Society. Copyright © American Chemical Society. However, no copyright claim is made to original U.S. Government works, or works produced by employees of any Commonwealth realm Crown government in the course of their duties.

Orientation of Organic Cations in Hybrid Inorganic-Organic Perovskite $CH_3NH_3PbI_3$ from Sub-atomic Resolution Single Crystal Neutron Diffraction Structural Studies

Yixin Ren,[†] Iain W. H. Oswald,[†] Xiaoping Wang,[‡,*] Gregory T. McCandless,[†] Julia Y. Chan[†,*]

[†]Department of Chemistry and Biochemistry, The University of Texas at Dallas, Richardson, Texas 75080, United States

[‡]Chemical and Engineering Materials Division, Neutron Sciences Directorate, Oak Ridge National Laboratory, Tennessee 39831, United States

Abstract

We report the crystal growth of well-faceted single crystals of methylammonium lead iodide, $CH_3NH_3PbI_3$, and detailed single crystal neutron diffraction structural studies aimed at elucidating the orientation of the methylammonium ($CH_3NH_3^+$) cation in the tetragonal and cubic phases of the hybrid inorganic-organic perovskite. Room temperature experiments reveal a tetragonal structure where the protonated amine substituent ($–NH_3^+$) of the cation is disordered in four positions, each preferentially located near the neighboring iodine of the [PbI_6] octahedra, while the methyl substituent ($–CH_3$) is disordered in eight positions located near the body position of the unit cell. High temperature experiments show a cubic structure where the cation aligns along the [011] (edge), the [111] (diagonal), and the [100] (face) directions of the unit cell. The resulting site occupancy ratio suggests the $CH_3NH_3^+$ cation resides primarily along the [011] direction, in agreement with reported DFT calculations. One important feature that was observed for both tetragonal and cubic structures measured at 295 K and 350 K, respectively, is the middle point of the C–N bond being located off-center from the high symmetry sites in the crystal structure, induced by the formation of hydrogen bond-like interactions between the $–NH_3^+$ substituent of the organic cation and the iodine atoms of [PbI_6] octahedra.

Introduction

The hybrid inorganic-organic $CH_3NH_3PbI_3$ perovskite is a promising material for photovoltaics, with conversion efficiencies exceeding 20%.[1-3] The positioning, orientation and rotational dynamics[4,5] of $CH_3NH_3^+$ cations have a direct impact on the electronic properties of the material and, therefore, a strong influence on photovoltaic performance.[2,3] Theoretical studies based on density functional theory (DFT) calculations have suggested that molecular rotations and orientation of the $CH_3NH_3^+$ cation can lead to a dynamic change of the band structure, possibly explaining the slow carrier recombination and the superior solar energy conversion efficiency of $CH_3NH_3PbI_3$.[6,7] For instance, in the cubic phase, calculations show when $CH_3NH_3^+$ cations orient along the [011] direction, an indirect band gap is present with an energy of 1.629 eV, while ordering along the [111] direction results in a direct gap of 1.611 eV.[6,8] Thus, determining the exact location of C, N, and H atoms in $CH_3NH_3PbI_3$ single crystals will allow one to resolve the details of the orientation of $CH_3NH_3^+$ cation in the crystal structure.

In previous structural studies using X-ray diffraction techniques, the best space group to model the structure has proven controversial for the tetragonal phase, adopted between 165 K and 330 K. Numerous structures have been reported using various space groups including *I*4*cm*,[9] *I*4/*m*,[1] and *I*4/*mcm*.[4,10] Some reported models omit the $CH_3NH_3^+$ cation altogether, highlighting the difficulty in accurately modeling the structure of this material. The controversial results surrounding the orientation of the $CH_3NH_3^+$ cation calls for accurate and in-depth structural studies of the $CH_3NH_3^+$ cation in single crystalline $CH_3NH_3PbI_3$. In this work, we report the high resolution structures of $CH_3NH_3PbI_3$ measured at 295 K and 350 K using the TOPAZ single crystal neutron diffractometer at the ORNL Spallation Neutron Source. Neutron diffraction is an excellent technique for investigating materials with similar atomic numbers such as carbon and nitrogen; additionally, hydrogen atoms can be identified definitively due to their negative scattering length. The TOPAZ instrument uses the neutron wavelength-resolved Laue technique for three-dimensional reciprocal space mapping, capable of measuring a structure at sub-atomic resolution. Our results reported herein based on data collected at 295 K (d_{min} = 0.59 Å) reveal that the protonated amine substituent of the $CH_3NH_3^+$ cation is disordered in four positions, while the methyl substituent is disordered in eight positions. Additionally, our results confirm a recent report using neutron powder diffraction that the best space group to model the tetragonal room temperature structure is *I*4/*mcm*.[11] Experiments on the high temperature cubic phase collected at 350 K (d_{min} = 0.58 Å) reveal that there still remains an orientational preference for the $CH_3NH_3^+$ cation, primarily aligned along the [011] direction.

An important feature revealed by our experiments for both tetragonal and cubic structures is the location of $CH_3NH_3^+$ cations being slightly off the body-center position, which is different from what has been reported in powder neutron diffraction data.[11] We believe the driving force for the $CH_3NH_3^+$ cation to move away from the ideal A-site is due to the formation of hydrogen bonds between the protonated amine ($–NH_3^+$) of the organic cation and the iodine atom of $[PbI_6]$ octahedra. This concept can be supported with static DFT calculations by the analysis of structural parameters such as the $NH_3^+\cdots I$ interatomic distances.[12]

Experimental Section

Synthesis.

Small crystals (< 1mm^3) of $CH_3NH_3PbI_3$ were prepared by following a similar method described by Poglitsch and Weber with a few modifications.[4] The following reagents: lead(II) acetate trihydrate ($Pb(CH_3COOH)_2·3H_2O$, 99%), hydriodic acid (HI, 57% w/w aq. soln., stabilized with 1.5% hypophosphorous acid), and methylamine (CH_3NH_2, 40% w/w aq. soln.) were used as received without further purification. $Pb(CH_3COOH)_2·3H_2O$ (9.7664 g, 0.02574 mol) was dissolved in 30.0 mL HI in a 50 mL round bottom flask. The reaction mixture was stirred for 15 min at 100 °C until all the solid was dissolved in the solution. To this solution, a mixture of 7.0 mL of HI and 2.5 mL (0.06407 mol) of CH_3NH_2 was added. The temperature was decreased to 75 °C to induce the saturation of the solute and allow the formation of small $CH_3NH_3PbI_3$ single crystals. Small, black, shiny crystals of $CH_3NH_3PbI_3$ were successfully grown in the bottom of the flask after one day.

For large $CH_3NH_3PbI_3$ single crystal growth, we have found a simplified synthetic method produces large crystals up to 5 mm in size synchronously in high synthetic yield (shown in Figure 1). A 15 mL aliquot of the mixed hot solution was transferred to a 20 mL vial, where the temperature of the solution was allowed to cool to 25 °C, and after 3-4 days multiple shiny single crystals with average dimensions of 3 x 4 x 4 mm^3 were grown. The reaction scheme is shown in Figure 2.

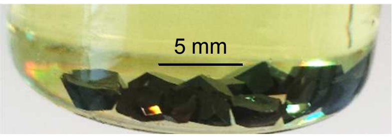

Figure 1. As grown well-faceted single crystals from a supersaturated solution at room temperature.

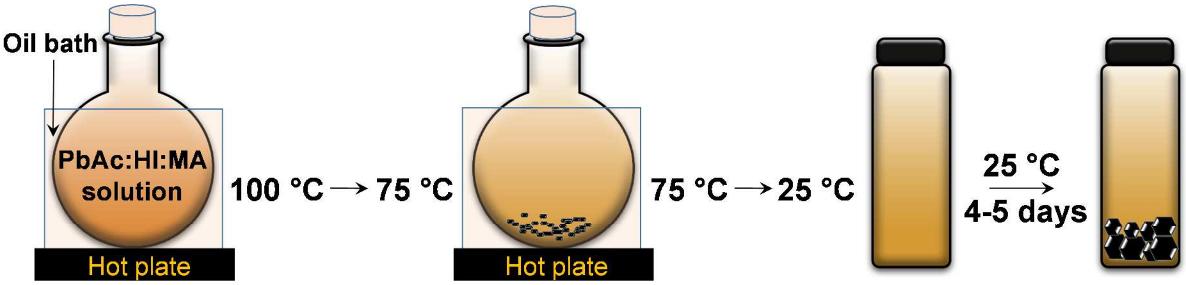

Figure 2. Schematic diagram of the crystallization process. PbAc = lead(II) acetate trihydrate, MA = methylamine.

Single Crystal Neutron Diffraction

Single crystal neutron diffraction was used to study the orientation and disorder of the methylammonium cation located between [PbI_6] octahedra in $CH_3NH_3PbI_3$ at the Spallation Neutron Source (SNS).[13] A single crystal with dimensions of 1.5 x 1.8 x 2.1 mm^3 was mounted onto a MiTeGen pin with superglue and positioned onto the goniometer. High resolution single-crystal neutron diffraction experiments were performed using the TOPAZ neutron time-of-flight single crystal Laue diffractometer. Data collections were conducted at 295 K and 350 K for the same single crystal sample using neutrons with wavelengths in the range of 0.4 to 3.3 Å. Sample orientations were optimized with CRYSTALPLAN.[14] Data were collected with 21 detectors and used 12 and 5 crystal orientations, respectively to ensure a good (> 98%) coverage and redundancy for each data collection, with collection times of approximately 2 h per sample orientation. The integrated raw Bragg intensities were obtained using the 3-*D* ellipsoidal *Q*-space integration method.[15] Data reduction including Lorentz, absorption, time-of-flight spectrum and detector efficiency corrections were carried with ANVRED3 program.[16] The reduced data were merged and saved in SHELX HKLF 2 format. Initial models were based on the single crystal X-ray diffraction refinement results, and the neutron modes were refined using SHELX2014.[17,18] Hydrogen atoms on methlyammonium were placed with the riding constraint HFIX 137 that allows for free rotation of the $–CH_3$ / $-NH_3$ groups along the C─N bond, but keeps the C─H/N─H bond distances and "idealized" tetrahedral angles fixed at default values. HFIX 137 instruction itself will not produce error estimates. Standard deviations of hydrogen bonding distances were estimated from an unconstrained refinement by combining HTAB with L.S. 1 DAMP 0 0 and MORE 3 instructions.[18,19] VESTA was used for 3D visualization of the difference Fourier maps to allow identification of structural disorder and regions of excess nuclear density.[19]

Tetragonal phase at 295 K structural refinement.

The structural model was initially refined with the Pb and I atom positions derived from our preliminary single crystal X-ray diffraction data. Initial refinements included the atomic positions and atomic displacement parameters (ADPs) for Pb and I. Due to the disorder observed at the position of C and N atoms, the SUMP command was applied, which restrains the atomic positions of the disorder sites. Additionally, a soft restraint (DFIX command) of the C─N bond length was applied to ensure the C─N bond is within the sum of their atomic radii. The tetragonal crystal forms twin domains, related by a 2-fold rotation about (1 -1 -2) reciprocal lattice direction of the tetragonal cell. The 2-fold symmetry corresponds to the (0 -1 -1) reciprocal lattice direction of the aristotype $Pm\bar{3}m$ cubic cell. Since the point group symmetry of the twin lattice differs from that of the tetragonal cell, the twin law can be classified as reticular pseudo-merohedric twin, with obliquity angle of 0.31° degrees calculated using the TwinRotMat program in Platon.[20] The corresponding TWIN command with the matrix transformation (-0.497 -0.503 -0.497, -0.503 -0.497 0.497, -1.005 1.005 -0.005) was applied in refinement of the neutron structure. The corresponding BASF parameter was refined to 0.20, indicating a second domain of 20% overall. The disordered $CH_3NH_3^+$ cation was assigned to a negative part number (part -1) to prevent bonds to symmetry generated atoms. In SHELX refinement, if the part number n is negative, special position constraints will be suppressed and all atoms are treated as if they were in general positions which [symmetry order] parameter = 1. Furthermore, the $CH_3NH_3^+$ cation resides near the 4*b* site with a D_{2d} symmetry [order 32/4 = 8]. The site symmetry is higher than that of the C_{3v} symmetry of methylammonium ($CH_3NH_3^+$), resulting in the disorder of the cation in four locations. The N1 atom located at the 16*l* Wyckoff site is supposed to have an order of 2 (32/16), but it was set to 1 in the crystallographic information file

(CIF), with the same being done for C atom C2 at 32*m* site. Therefore, the occupancies of C, N and H atoms in the crystal structure were fixed to 0.125 to match the unit cell contents of Pb atoms located at the 4*c* site with a symmetry order 8, consisting with the formula $CH_3NH_3Pb_1I_3$ with Z =4. Final cycles of the *I*4/*mcm* refinement statistics indicate a good fit to the observed data (R_1 = 6.0%, wR_2 = 15.0%, GOF = 1.04). The structural refinement data and atomic coordinates with ADPs are summarized in Table 1 and 2. The selected bond lengths and angles of the final structural refinement are summarized in Table 3.

Cubic phase at 350 K structural refinement. The highest temperature phase T > 327 K was confirmed to be cubic, consistent with previous reports. The refinement of the cubic structure used the model in space group $Pm\overline{3}m$ with Pb and I atoms located at (0,0,0) and (0,0,1/2), as that previously described from powder X-ray diffraction data.[1] The site occupancies of the disordered $CH_3NH_3^+$ moieties were refined using a model with the cation aligned along the [111], [100], and the [011] directions of the unit cell. Final cycles of refinement converged to R_1 = 4.9%, wR_2 = 7.5%, GOF = 1.28, with the resulting site occupancy ratio 0.143:0.187:0.670, indicating that the $CH_3NH_3^+$ cation resides primarily along the [011] direction. Full crystallographic details regarding the structural refinement are shown in Table 1. The atomic coordinates with anisotropic displacement parameters and selected bond lengths are summarized in Table 4 and 5.

CCDC 1470054-1470055 contain the supplementary crystallographic data for $CH_3NH_3PbI_3$ measured at 295 K and 350 K. These data can be obtained free of charge from The Cambridge Crystallographic Data Centre via www.ccdc.cam.ac.uk/data_request/cif.

Results and Discussion

Numerous single crystal X-ray diffraction experiments have been unable to determine the location of the $CH_3NH_3^+$ cation. Additionally, when the location and orientation were reported, these results have not been consistent with other studies. Our results using single crystal neutron diffraction data measured at 295 K and 350 K have led to a structural model with detailed structural information for the $CH_3NH_3^+$ cation in the tetragonal and cubic phases. Tables 1-5 include details regarding the structural model, atomic positions, pertinent atomic distances, and angles. The relatively large differences between neutron scattering lengths of C and N (6.646 fm and 9.360 fm, respectively), overcome the problems experienced when modeling the C/N disorder via X-ray diffraction.[21] Furthermore, single crystals provide high resolution data necessary for observing the fine structural details related to the methylammonium cation.

Structural refinements of the tetragonal phase using various space groups including previously reported *I*4*cm*, *I*4/*m* and *I*4/*mcm* were performed.[1,22,9] All three space groups gave reasonable statistics of R = 6%, 8.5%, 15% for *I*4/*mcm*, *I*4*cm*, and *I*4/*m,* respectively. Structurally, the three models were very similar in regard to the $[PbI_6]$ octahedra structure. The distorted bond angles between I2─Pb1─I2 were observed in all three cases. It was also found necessary to restrain the C-N bond distance to a realistic value of 1.469 Å to prevent the model from diverging, while still allowing this value to refine. However, doing so in space groups *I*4*cm* and *I*4/*m* resulted in the presence of non-positive definites (NPDs) with this restraint. On the other hand, no NPDs were observed for using space group *I*4/*mcm*, yielding a refined C–N bond length of -1.467(3) Å, same to the bond length reported for methylammonium in $CH_3NH_3I{\cdot}H_2O$.[23] Therefore, we believe that *I*4/*mcm* is indeed the best space group to represent the structure of $CH_3NH_3PbI_3$, consistent with the reported neutron powder diffraction data.[11]

Table 1. Crystal Data and Structure Refinement for $CH_3NH_3PbI_3$ Obtained from Neutron Diffraction

	295 K	350 K
Crystal system	Tetragonal	Cubic
Wavelength (Å)	0.6-3.3	0.6-3.3
Space group	$I4/mcm$	$Pm\bar{3}m$
Unit cell dimensions (Å)	a = 8.8796(6)	a = 6.315(3)
	c = 12.6266(18)	
Volume (Å^3)	995.6(2)	251.8(4)
Z	4	1
Density (calculated) (g cm^{-1})	4.136	4.088
Absorption coefficient (mm^{-1})	0.0654 + 0.05078 λ	
$F(000)$	1040	260
Crystal size (mm^3)	1.5 x 1.8 x 2.1	1.5 x 1.8 x 2.1
Theta range for data collection (°)	7.4 to 78.5	7.9 to 78.1
Index ranges	$-13 \leq h \leq 14$	$-9 \leq h \leq 8$
	$-12 \leq k \leq 14$	$-10 \leq k \leq 10$
	$-16 \leq l \leq 20$	$-10 \leq l \leq 10$
Reflections collected	3825	968
Independent reflections	414	139
R_{int}	0.142	0.164
Refinement method	Full-matrix least-squares on F^2	
Data / restraints / parameters	414 / 71 / 67	139 / 10 / 33
Goodness-of-fit on F^2	1.04	1.28
$R_1[F^2 > 2\sigma(F^2)]^a$	0.060	0.049
$wR_2(F_2)^b$	0.150	0.075
Extinction coefficient	0.11(3)	1.3(3)
Largest diff. peak and hole (fm. Å^{-3})	0.72 and -0.42	0.28 and -0.51

$^a R_1(F) = \Sigma||F_o| - |F_c||/\Sigma|F_o|$. $^b wR_2(F^2) = [\Sigma[w(F_o^2 - F_c^2)^2]/\Sigma[w(F_o^2)^2]]^{1/2}$

Table 2. Atomic Coordinates and Equivalent Isotropic Displacement Parameters for *I*4/*mcm*

atom	Wyckoff Site	*x*	*y*	*z*	Occ	U_{eq} (Å^2)^a
Pb1	4*c*	1/2	1/2	1/2	1	0.0262(4)
I1	4*a*	1/2	1/2	3/4	1	0.069(2)
I2	8*h*	0.7868(4)	0.2868(4)	1/2	1	0.0686(15)
N1	32*m*	0.0696(8)	0.4304(8)	0.2858(10)	1/8	0.085(3)
H1A	32*m*	0.1649	0.4934	0.3002	1/8	0.103(7)
H1B	32*m*	0.0952	0.3444	0.2342	1/8	0.097(7)
H1C	32*m*	0.0294	0.3866	0.3556	1/8	0.092(7)
C2	32*m*	-0.047(2)	0.527(2)	0.2385(15)	1/8	0.090(4)
H2A	32*m*	-0.0757	0.6133	0.2925	1/8	0.104(8)
H2B	32*m*	-0.1433	0.4610	0.2213	1/8	0.096(7)
H2C	32*m*	-0.0049	0.5750	0.1676	1/8	0.109(8)

$^a U_{eq}$ is defined as one-third of the trace of the orthogonalized U_{ij} tensor.

Table 3. Selected Bond Lengths and Angles for $CH_3NH_3PbI_3$ in the Tetragonal Phase, *I*4/*mcm* at 295 K

Bond	Bond length (esd) (Å)	Angle	(°)
Pb–I1 x 2	3.1567(5)	Pb–I1–Pb	180.0
Pb–I2 x 4	3.1732(8)	Pb–I2–Pb	163.3(2)
C–N	1.467(3)		
N–$H_{(1A)}$···I1	3.04(7)		
N–$H_{(1C)}$···I2	2.96(5)		
C–$H_{(2C)}$···I2	3.07(6)		

Table 4. Atomic Coordinates and Equivalent Isotropic Displacement Parameters for $Pm\bar{3}m$ at 350K

atom	Wyckoff Site	*x*	*y*	*z*	Occ	U_{eq} (Å^2)^a
Pb1	1*b*	1/2	1/2	1/2	1	0.0301(3)
I1	3*d*	0	0	1/2	1	0.1219(1)
N1	8*g*	05890(13)	0.5890(13)	0.5890(13)	0.00297(1)	0.099(5)
H1A	48*n*	0.7171	0.5027	0.6414	0.00297(1)	0.092(5)
H1B	48*n*	0.5027	0.6414	0.7171	0.00297(1)	0.092(5)
H1C	48*n*	0.6414	0.7171	0.5027	0.00297(1)	0.092(5)
C1	8*g*	0.4544(13)	0.4544(13)	0.4544(13)	0.00297(1)	0.076(5)
H1D	48*n*	0.3808	0.3367	0.5488	0.00297(1)	0.092(5)
H1E	48*n*	0.5488	0.3808	0.3367	0.00297(1)	0.092(5)
H1F	48*n*	0.3367	0.5488	0.3808	0.00297(1)	0.092(5)
N2	6*f*	0.653(2)	1/2	1/2	0.00038(8)	0.092(5)
H2A	48*n*	0.7069	0.4187	0.6305	0.00038(8)	0.092(5)
H2B	48*n*	0.7069	0.6537	0.5052	0.00038(8)	0.092(5)
H2C	48*n*	0.7069	0.4277	0.3643	0.00038(8)	0.092(5)
C2	6*f*	0.420(2)	1/2	1/2	0.00038(8)	0.076(5)
H2D	48*n*	0.3636	0.5759	0.6389	0.00038(8)	0.092(5)
H2E	48*n*	0.3636	0.3418	0.4963	0.00038(8)	0.092(5)
H2F	48*n*	0.3636	0.5823	0.3648	0.00038(8)	0.092(5)
N3	12*j*	1/2	0.6054(9)	0.6054(9)	0.01397(1)	0.099(5)
H3A	48*n*	0.4712	0.7506	0.5370	0.01397(1)	0.092(5)
H3B	48*n*	0.6452	0.6081	0.6795	0.01397(1)	0.092(5)
H3C	48*n*	0.3836	0.5727	0.7419	0.01397(1)	0.092(5)
C3	12*j*	1/2	0.4402(9)	0.4402(9)	0.01397(1)	0.076(5)
H3D	48*n*	0.6032	0.4854	0.3158	0.01397(1)	0.092(5)
H3E	48*n*	0.3445	0.4214	0.3798	0.01397(1)	0.092(5)
H3F	48*n*	0.5523	0.2950	0.5062	0.01397(1)	0.092(5)

$^a U_{eq}$ is defined as one-third of the trace of the orthogonalized U_{ij} tensor.

Table 5. Selected Bond Lengths for $CH_3NH_3PbI_3$ in the Cubic Phase, $Pm\bar{3}m$ at 350 K

Bond	Bond length (esd) (Å)
Pb─I x 6	3.1575(15)
C1─N1	1.472(8)
C2─N2	1.471(9)
C3─N3	1.475(7)
N–H1···I1	3.05(7), 3.10(5)

Figure 3a shows the regions of positive nuclear density in yellow arising from the carbon and nitrogen atoms. The irregular shape of the density is elongated in four directions extending from the interior indicating that either the methyl ($–CH_3$) or protonated amine ($–NH_3^+$) substituent are orientated toward the [PbI_6] octahedra. The positive nuclear density is surrounded by a sphere of negative nuclear density due to the presence of protons, which are represented in blue as shown in Figure 3b. Closer inspection of the positive nuclear density reveals a larger density at the four exterior termini nearest the [PbI_6] octahedra. This signifies the protonated amine substituent, which has a larger scattering factor due to the presence of nitrogen (versus carbon), occupies these four positions. This is most likely due to the N–H bonds being more polar than the C–H bonds, where the majority of the electronegativity is localized on the nitrogen atom, favoring weak hydrogen bonding between the protonated amine ($–NH_3^+$) substituent and the electronegative iodine atoms of the neighboring [PbI_6] octahedra. This interaction prevents the orientation of the $CH_3NH_3^+$ cation from being completely random, essentially locking the location of the protonated amine substituent. The difference Fourier map reveals the remaining positive nuclear density surrounding the 4*b* Wyckoff sites is due to the carbon atoms of the methyl substituent. We initially attempted to refine the model with the carbon atom constrained to the 16*l* Wyckoff site where the N and C positions were assigned to (x, 1/2+x, z) with z equal to 0.2855 for N and 0.2384 for C. This was based on the results of the previously reported neutron powder diffraction studies of $CH_3NH_3PbI_3$ perovskite;[11] however, this resulted in anomalously large ADPs, as well as significantly poorer refinement statistics. Therefore, the position of the carbon atom was allowed to freely refine, revealing the actual location to be slightly off the ideal 16*l* Wyckoff site. This slight change in position generates two possible carbon positions through a mirror plane, resulting in the C termini in $CH_3NH_3^+$ to be disordered in eight positions instead of 4 (Figure 4). This result is different from that of the reported neutron powder diffraction studies where the carbon atom was located exactly at the 16*l* Wyckoff site; however, structural details of the tetragonal phase were reported at 180 K, well below the temperature of our experiment conducted at 295 K. This could support the hypothesis that the splitting observed in our model is due to thermal disorder, as in the case of the neutron powder diffraction experiments collected at 180 K, the thermal energy is minimized, resulting in the carbon atom to be located at the ideal 16*l* Wyckoff site.

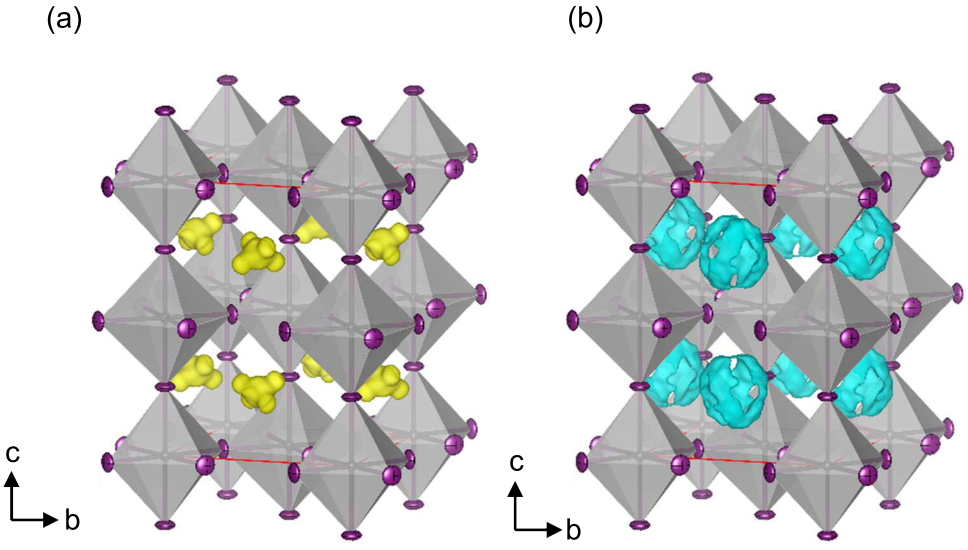

Figure 3. 3D difference Fourier maps from single crystal neutron diffraction data for $CH_3NH_3PbI_3$, (a) showing the region of positive (yellow) nuclear density indicates the disorder of the $CH_3NH_3^+$ cation, (b) Showing the region of negative (blue) nuclear indicates a highly disordered arrangement of the hydrogen atoms.

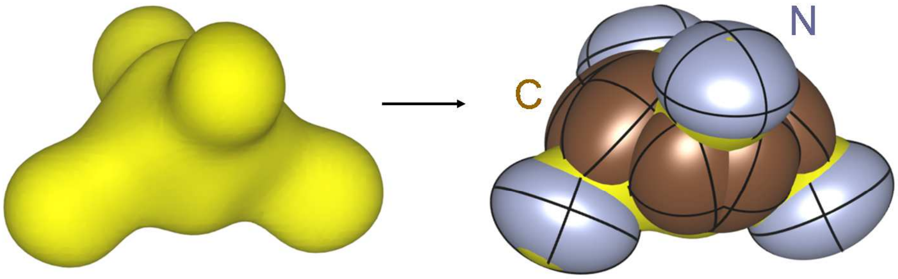

Figure 4. The positive nuclear scattering has a larger value at the four exterior lobes indicating the presence of nitrogen (shown in silver). The central disordered area has a lower scattering factor due to the presence of carbon (shown in brown) that is disordered to generate a total of eight positions.

As mentioned previously, large, spherical, negative nuclear scattering density was observed surrounding the interior positive nuclear scattering density. This density is associated with the presence of hydrogen atoms, having a negative scattering factor of -3.739 fm. The hydrogen atoms are highly disordered and can be visualized explicitly in the difference Fourier maps in Figure 3b. Each of the four possible $–NH_3^+$ positions (Figure 5a) generate two N–H···I contacts by symmetry with a distance of 2.96(5) Å. This distance is shorter than all other H···I contacts, including contacts with the $–CH_3$ substituent where the shortest C–H···I distance is 3.07(6) Å. Figure 5b shows one of the four possible orientations of the $CH_3NH_3^+$ cation with a dashed line indicating the shortest N–H···I contact. This is shorter than the distance reported using neutron powder diffraction at 180 K, which was 3.184(12) Å. It should also be noted that the C–N–H angles (109.5 °) in our model are larger than those reported in the neutron powder diffraction study (~ 84.14 °).[11] Further, the bond distances and angles closely resembles that of ammonium iodide (NH_4I),[24] where hydrogen-bonding plays an important role for the structural stabilization. The detailed hydrogen bond lengths and angles of the neutron diffraction data are given in Table 6.

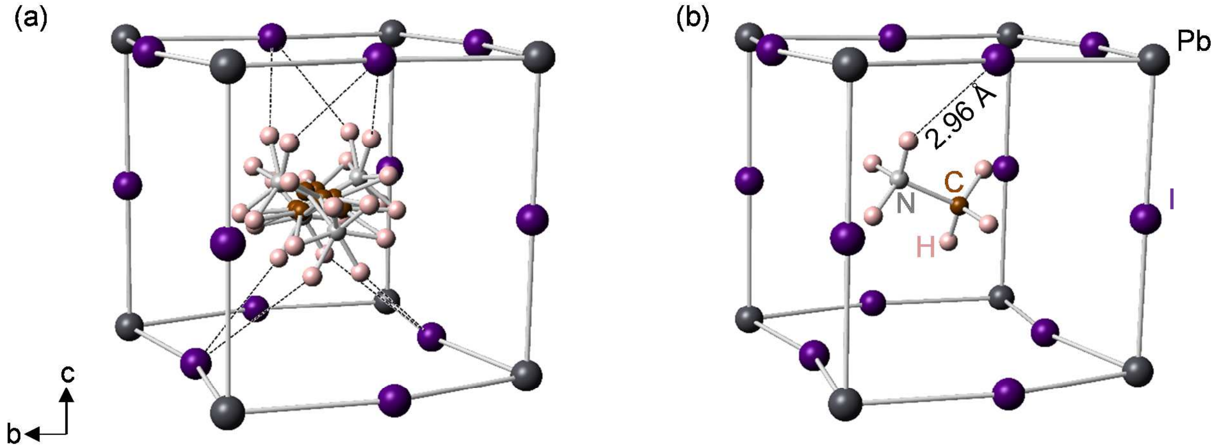

Figure 5. Left: The disordered methylammonium cation is shown with each N–H···I contact. Right: A single $CH_3NH_3^+$ cation is shown with the disordered hydrogen atoms surrounding both N and disordered C atom. Pb-grey, I-black, N-grey, C-brown, H-pink. The shortest I···H contact is shown (dotted line).

Table 6. Hydrogen Bonds for *I*4/*mcm* (Å and °)

D–H···*A*	d(*D*–H)	d(H···*A*)	d(*D*···*A*)	bond angle (*D*H*A*)
$N–H_{(1A)}···I_{(1)}$	1.03(6)	3.04(7)	3.898(7)	141.1
$N–H_{(1C)}···I_{(2)}$	1.03(6)	2.96(5)	3.90 5(11)	152.8

"*D*" represents donor and "*A*" represents acceptor.

The $[PbI_6]$ octahedral framework is found to be distorted and tilted in the tetragonal phase of $CH_3NH_3PbI_3$ that can be represented using Glazer notation $a^0a^0c^-$.[25] The notation "+" or "-" represents in-phase or out-of phase, respectively, and are applied when describing the tilt or rotations about the three I–Pb–I axes along the crystallographic *a*, *b*, *c* axes. The tilting angle of 16.75° results in an out-of-phase rotation of the $[PbI_6]$ octahedra along the *c*-axis, adopting the tetragonal *I*4/*mcm* space group.

With increasing temperature, $CH_3NH_3PbI_3$ undergoes a phase transition from the tetragonal to cubic phase at 327 K, with a concomitant increase in $CH_3NH_3^+$ cation disorder. Our experiment at 350 K was successfully modeled using space group $Pm\bar{3}m$ with good statistical values ($R_1 = 0.049$, $wR_2 = 0.075$). Through careful analysis of the 3D nuclear difference Fourier maps for $CH_3NH_3^+$ at 350 K (Figure 6), we have found that the middle point of C–N bond is located off-center from the ideal A-site of the perovskite structure in the crystal structure. This is evident in Figure 6a and b, where the positive nuclear density in yellow represents the center of the $CH_3NH_3^+$ cation. The surrounding hydrogen atoms are highly disordered, as shown in nuclear difference Fourier maps for $CH_3NH_3^+$ in Figure 6c, where blue region indicate the negative nuclear density due to the hydrogen atoms. The final model resulted in the $CH_3NH_3^+$ cation being directed toward the face of the unit cell, disordered over six positions with weak N–H···I interaction having hydrogen bond distances of 3.05 (7) Å and 3.10(5 Å (Figure 6d). All Pb–I–Pb angles are linear resulting in a perfect octahedron, further indicating the weaker N–H···I interaction, as compare to the tetragonal phase, where the stronger N–H···I interaction resulted in the distortion and tilt of the [PbI_6] octahedra.

Although a greater amount of disorder is present in the cubic phase than that in the tetragonal phase, our data reveal that the disordered $CH_3NH_3^+$ cation preferentially aligns along the [111], [100] and [011] directions. Furthermore, these orientations have site occupancy ratios of 0.143 : 0.187 : 0.670 respectively, suggesting that the $CH_3NH_3^+$ cation resides primarily along the [011] direction at high temperature. These results are in accordance with previous DFT calculations that suggest the structure with the $CH_3NH_3^+$ cation oriented along the [011] direction lies at an energetic minimum, albeit by only about 20 meV.[6,8] The shallow energetic minima corresponding to the various orientations could explain why our model has three primary orientations, with a slight preference to align along the [011] direction. Additionally, the calculations also predict a slight distortion of the surrounding [PbI_6] octahedra when oriented along the [011] direction, breaking the perfect 180° I–Pb–I angle. In our model, we observe large, pancake-shaped thermal ellipsoids for iodine (Figure 6d), indicating the actual location of the iodine atoms may in fact be off the ideal 3*d* Wyckoff position. For the purpose of comparing our results with the DFT calculations, we intentionally moved I atom slightly off the 3*d* Wyckoff position to allow it to freely refine (Details of the structure including hydrogen bond distances with I moved off the axial position can be found in supporting information). Indeed, the refined location of the I atom is slightly off of the edge of the unit cell with no significant statistical change to the model (R_1 = 0.048 and wR_2 = 0.0721), in good agreement with those predicted by calculations.

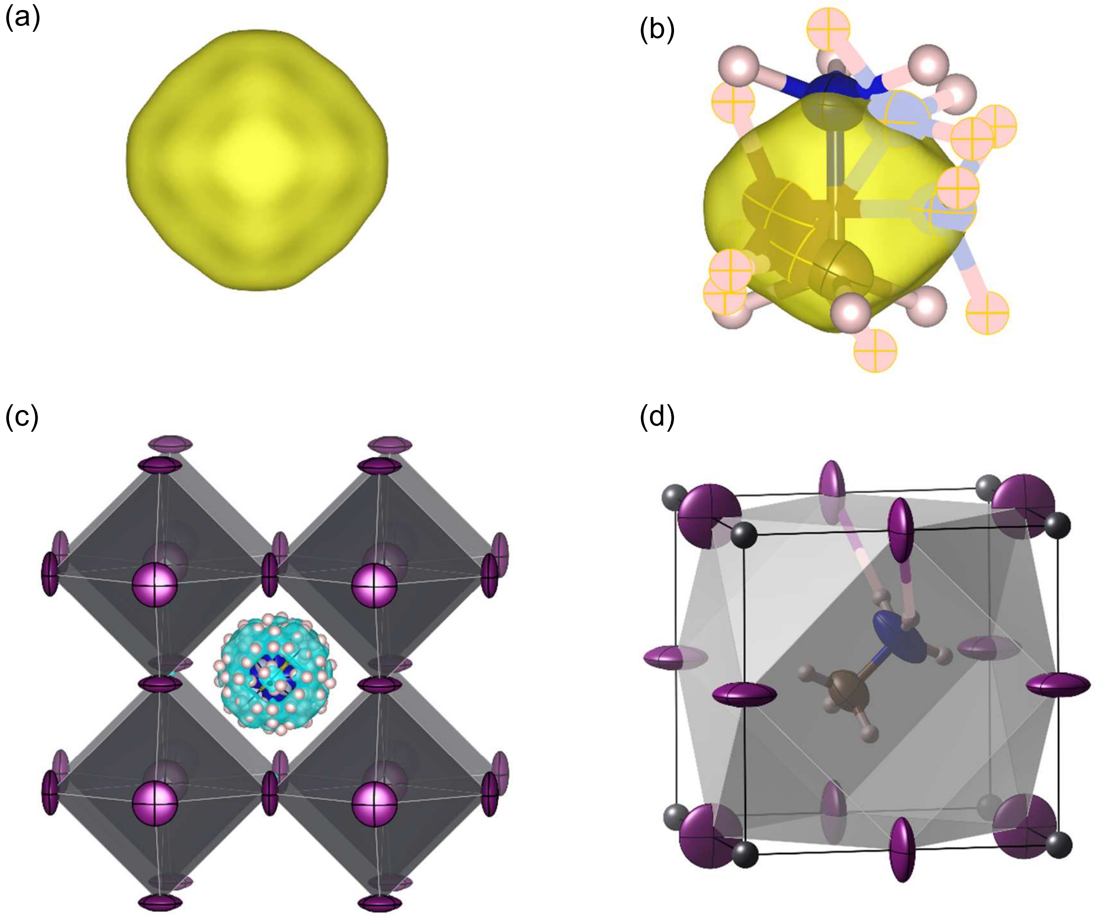

Figure 6. 3D Nuclear difference Fourier maps for $CH_3NH_3^+$ at 350 K. (a) The region of positive (yellow) nuclear density indicates disorder of C and N atoms in $CH_3NH_3^+$, (b) Location of disordered CN groups (N blue, C brown) and H atoms from refinement of the neutron structure (c) View of the structure of $CH_3NH_3PbI_3$ showing the region of negative (blue) nuclear and a highly disordered arrangement of the hydrogen atoms. (d) Location of $CH_3NH_3^+$ with the CN bond aligned along [011] direction.

Conclusions

We report a detailed description of the crystal structure of $CH_3NH_3PbI_3$, including the orientation, location and disorder of the methylammonium cation within the $[PbI_6]$ octahedra of by using single crystal neutron diffraction. The tetragonal phase at 295 K was confirmed to be best modelled in *I*4/*mcm*. The $CH_3NH_3^+$ cations are disordered such that there are four possible orientations of the $–NH_3^+$ substituent being on the extremity nearest the neighboring I atom. Conversely, the methyl substituent was found to have eight possible positions as opposed to the four of the protonated amine substituent due to a greater ability to move as there are no means of stabilizing its location. The high temperature (350 K) cubic phase was successfully modelled using space group $Pm\bar{3}m$. We have sucessfully located the $CH_3NH_3^+$ cation and discerned the C and N atoms. More importantly, our data reveal a key feature of the orientation of the $CH_3NH_3^+$ cation where the $CH_3NH_3^+$ cation resides mainly along [011] direction, which is in good agreement with reported DFT calculations. These findings provide important structural information for both the tetragonal and cubic phases, and will help in understanding the origin of the excellent photovoltaic performance of this material.

Supporting Information

Crystallographic information files (CIF) of $CH_3NH_3PbI_3$ at 295 K and 350 K. Additional 3D difference Fourier maps for the refined structure of $CH_3NH_3PbI_3$ at 295 K presented in Figures S1-S3. This material is available free of charge via the Internet at http://pubs.acs.org.

Author Information

Corresponding Author

*E-mail: Julia.Chan@utdallas.edu. Tel: (972)883-3595.
*E-mail: wangx@ornl.gov. Tel: (865)200-2500.

Notes

The authors declare no competing financial interest.
All authors contributed equally to this work.

Acknowledgements

JYC acknowledges NSF-DMR-1360863 for partial funding of this work. Neutron single crystal diffraction measurements were performed at the Spallation Neutron Source, which is sponsored by the Division of Scientific User Facilities, Office of Basic Energy Sciences, US Department of Energy, under Contract No. DE.-AC05-00OR22725 with UT-Battelle, LLC.

References

(1) Baikie, T.; Fang, Y.; Kadro, J. M.; Schreyer, M.; Wei, F.; Mhaisalkar, S. G.; Graetzel, M.; White, T. J. *J. Mater. Chem. A.* **2013**, *1*, 5628.

(2) Green, M. A.; Ho-Baillie, A.; Snaith, H. J. *Nat. Photonics.* **2014**, *8*, 506.

(3) Stoumpos, C. C.; Kanatzidis, M. G. *Acc. Chem. Res.* **2015**, *48*, 2791.

(4) Poglitsch, A.; Weber, D. *J. Chem. Phys.* **1987**, *87*, 6373.

(5) Wasylishen, R. E.; Knop, O.; Macdonald, J. B. *Solid State Commun.* **1985**, *56*, 581.

(6) Motta, C.; El-Mellouhi, F.; Kais, S.; Tabet, N.; Alharbi, F.; Sanvito, S. *Nat Commun* **2015**, *6*, 7026.

(7) Berdiyorov, G. R.; El-Mellouhi, F.; Madjet, M. E.; Alharbi, F. H.; Rashkeev, S. N. *Appl. Phys. Lett.* **2016**, *108*, 053901.

(8) Motta, C.; El-Mellouhi, F.; Kais, S.; Tabet, N.; Alharbi, F.; Sanvito, S. *Nat Commun* **2015**, *6*.

(9) Dang, Y.; Liu, Y.; Sun, Y.; Yuan, D.; Liu, X.; Lu, W.; Liu, G.; Xia, H.; Tao, X. *CrystEngComm.* **2015**, *17*, 665.

(10) Kawamura, Y.; Mashiyama, H.; Hasebe, K. *J. Phys. Soc. Jpn.* **2002**, *71*, 1694.

(11) Weller, M. T.; Weber, O. J.; Henry, P. F.; Di Pumpo, A. M.; Hansen, T. C. *Chem. Comm.* **2015**, *51*, 4180.

(12) Quarti, C.; Grancini, G.; Mosconi, E.; Bruno, P.; Ball, J. M.; Lee, M. M.; Snaith, H. J.; Petrozza, A.; Angelis, F. D. *J. Phys. Chem. Lett.* **2014**, *5*, 279.

(13) Hoffman, C.; Wang, X. P. *https://neutrons.ornl.gov/topaz.*

(14) Zikovsky, J.; Peterson, P. F.; Wang, X. P.; Frost, M.; Hoffmann, C. *J. Appl. Cryst.* **2011**, *44*, 418.

(15) Schultz, A. J.; Jorgensen, M. R. V.; Wang, X.; Mikkelson, R. L.; Mikkelson, D. J.; Lynch, V. E.; Peterson, P. F.; Green, M. L.; Hoffmann, C. M. *J. Appl. Cryst.* **2014**, *47*, 915.

(16) Schultz, A. J.; Srinivasan, K.; Teller, R. G.; Williams, J. M.; Lukehart, C. M. *J. Am. Chem. Soc.* **1984**, *106*, 999.

(17) Sheldrick, G. M. *Acta. Cryst. A.* **2008**, *64*, 112.

(18) Gruene, T.; Hahn, H. W.; Luebben, A. V.; Meilleur, F.; Sheldrick, G. M. *J. Appl. Cryst.* **2014**, *47*, 462.

(19) Momma, K.; Izumi, F. *J. Appl. Cryst.* **2011**, *44*, 1272.

(20) Spek, A. *J. Appl. Cryst.* **2003**, *36*, 7.

(21) Sears, V. F. *Neutron News.* **1992**, *3*, 26.

(22) Stoumpos, C. C.; Malliakas, C. D.; Kanatzidis, M. G. *Inorg. Chem.* **2013**, *52*, 9019.

(23) Hao, F.; Stoumpos, C. C.; Liu, Z.; Chang, R. P. H.; Kanatzidis, M. G. *J. Am. Chem. Soc.* **2014**, *136*, 16411.

(24) Kozlenko, D. P.; Savenko, B. N.; Glazkov, V. P.; Somenkov, V. A.; Hull, S. *Physica B.* **2000**, *276–278*, 226.

(25) Glazer, A. *Acta. Crystallogr., Sect. B.* **1972**, *28*, 3384.

For TOC Only

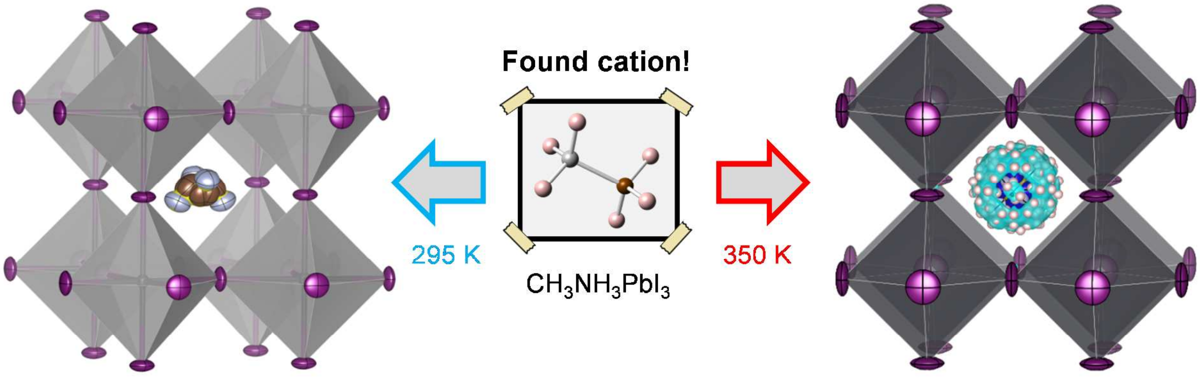

Orientation of Organic Cations in Hybrid Inorganic-Organic Perovskite CH$_3$NH$_3$PbI$_3$ from Sub-atomic Resolution Single Crystal Neutron Diffraction Structural Studies

Yixin Ren, Iain W. H. Oswald, Xiaoping Wang, Gregory T. McCandless, Julia Y. Chan

Synopsis:

Sub-atomic resolution single crystal neutron diffraction revealed off-center placement and orientation of the disordered methylammonium cation in the hybrid organic-inorganic perovskite CH$_3$NH$_3$PbI$_3$ in the room temperature (295 K) tetragonal phase and the high temperature (350 K) cubic phase.